
Adaptive analysis based on error estimation for nonlocal damage models

Antonio Rodríguez-Ferran — Ivan Arbós — Antonio Huerta

*Departament de Matemàtica Aplicada III, E.T.S. de Ingenieros de Caminos
Edifici C2, Campus Nord, Universitat Politècnica de Catalunya
E-08034 Barcelona, Spain*

{antonio.rodriguez-ferran,antonio.huerta}@upc.es

ABSTRACT. An adaptive finite element strategy for nonlocal damage computations is presented. The proposed approach is based on the combination of a residual-type error estimator and quadrilateral h -remeshing. A distinctive feature of the error estimator is that it consists in solving simple local problems over elements and so-called patches. The paper focuses on how the nonlocality of the constitutive model should be accounted for when solving these local problems. It is shown that the nonlocal damage models must be slightly modified. The resulting adaptive strategy is illustrated by means of some numerical examples involving the single-edge notched beam test.

RÉSUMÉ. On présente une stratégie adaptative par éléments finis pour des calculs avec endommagement non local. La méthode qu'on propose combine un estimateur d'erreur résiduel avec un raffinement de type h pour des éléments quadrilatères. Une des caractéristiques principales de cet estimateur est que l'on résout des problèmes locaux et simples, d'abord sur les éléments et, ensuite, sur des domaines que l'on appelle "patches". L'article est consacré à la description du traitement non local du problème.

On montre ainsi que la loi de comportement d'endommagement non local doit être légèrement modifiée. La stratégie adaptative qui s'en déduit est utilisée dans des exemples numériques simulant le test de la poutre entaillée ("single-edge notched beam").

KEYWORDS: Damage models; Nonlocal models; Error estimation; Adaptivity; Quasi-brittle materials; Single-edge notched beam

MOTS-CLÉS : Modèles d'endommagement ; modèles non locaux ; estimation d'erreur ; adaptativité ; matériaux fragiles ; poutre entaillée

1. Introduction

Damage models are nowadays a standard approach to model the failure of concrete and other quasi-brittle materials [LEM 90]. To avoid the pathological mesh dependence of numerical simulations carried out with local models, various regularisation techniques may be used [BOR 93]. One possibility, considered in this work, is the use of nonlocal damage models [PIJ 87, BAŽ 88, MAZ 89]. The basic idea of nonlocal models is that the damage parameter that describes the loss of stiffness depends on the strain state in a neighbourhood (associated to a characteristic length) of the point under consideration.

To ensure the quality of the finite element solution, an adaptive strategy based on error estimation was recently proposed by the authors [ROD 00]. A salient feature of the approach proposed in that reference is the extension of an existing residual-type nonlinear error estimator [DÍE 98, HUE 00] to the context of nonlocal damage models, where tangent stiffness matrices are not readily available.

Attention is focused here on the fact that the error estimator is based on local computations over elements and so-called patches. It will be shown that it is important to account for the nonlocality of the damage model when solving these local problems. This leads to a slight modification of the nonlocal damage model to be used during error estimation.

An outline of paper follows. Nonlocal damage models are briefly reviewed in section 2. Section 3 is devoted to the error estimator. After reviewing its main ingredients in section 3.1, section 3.2 discusses the required modification of the damage model so that its nonlocality is taken into account during error estimation. The resulting adaptive strategy is illustrated in section 4 by means of two numerical examples involving the single-edge notched beam test. The concluding remarks of section 5 close the paper.

2. Nonlocal damage models

The basic features of nonlocal damage models are briefly reviewed in this section. For the sake of clarity, only isotropic elastic-damage models are considered. These simple models are sufficient to illustrate how the error estimator based on local computations takes into account the nonlocality of the model. However, the approach can be extended to more complex nonlocal damage models, incorporating, for instance, anisotropy and/or coupling with plasticity [MAZ 89].

The loss of stiffness associated to mechanical degradation of the material is represented by a parameter D , according to

$$\boldsymbol{\sigma} = (1 - D)\mathbf{C} : \boldsymbol{\varepsilon}, \quad [1]$$

where $\boldsymbol{\sigma}$ and $\boldsymbol{\varepsilon}$ are respectively the Cauchy stress tensor and the small strain tensor, and \mathbf{C} is the tensor of elastic moduli (E : Young's modulus; ν : Poisson's coefficient).

Parameter D ranges between 0 (virgin material, with elastic stiffness) and 1 (completely damaged material, with no stiffness). For computational purposes, an upper bound of $D_{\max} = 0.99999$ is set. In this manner, zero stiffness is avoided and it is not necessary to remove the fully damaged elements from the mesh.

It is assumed that D depends on a state variable Y , which in turn depends on the strains:

$$Y = Y(\boldsymbol{\varepsilon}). \quad [2]$$

The basic idea of nonlocal damage models is averaging the state variable Y in the neighbourhood of each point. In this manner, the *nonlocal* state variable \tilde{Y} is obtained:

$$\tilde{Y} = \int_V \alpha(d)Y dV / \int_V \alpha(d)dV. \quad [3]$$

The weight function α , which depends on the distance d to the point under consideration, is typically the Gaussian

$$\alpha(d) = \exp \left[- \left(\frac{2d}{l_c} \right)^2 \right], \quad [4]$$

where the characteristic length l_c is a material parameter of the nonlocal damage model, which acts as a localization limiter and can be associated to the grain size [PIJ 91]. The nonlocal state variable drives the evolution of damage,

$$D = D(\tilde{Y}). \quad [5]$$

Damage starts above a threshold Y_0 (that is, $D = 0$ for $\tilde{Y} \leq Y_0$) and it cannot decrease (that is, $\dot{D} \geq 0$).

To define a particular model, it is necessary to specify the definition of the state variable, equation [2], and the evolution law for damage, equation [5].

In the modified von Mises model [VRE 95] Y depends on the first strain invariant I_1 , the second deviatoric strain invariant J_2 and the ratio k of compressive strength to tensile strength. Regarding the damage evolution for $\tilde{Y} > Y_0$, an exponential law [PIJ 91, ASK 00] is used. The modified von Mises model is summarized in table 1. More details about this model can be found in [VRE 95, PEE 98].

3. The error estimator

In order to control the finite element discretization errors, an adaptive strategy is employed [ROD 00]. It is based on the combination of a residual-type error estimator [DÍE 98, HUE 00] and h -remeshing. The error distribution is computed with the error estimator and translated into desired element sizes with a so-called optimality criterion [DÍE 99]. An unstructured quadrilateral mesh generator [SAR 00] is then used to build a mesh with the desired sizes. This iterative process stops (typically after 2 to 4 iterations) when the relative error of the solution (i.e. energy norm of the error divided by energy norm of the solution) is below a prescribed threshold set a priori.

$$\text{State variable: } Y = \frac{k-1}{2k(1-2\nu)} I_1 + \frac{1}{2k} \sqrt{\left(\frac{k-1}{1-2\nu} I_1\right)^2 + \frac{12k}{(1+\nu)^2} J_2}$$

$$\text{Damage evolution: } D = 1 - \frac{Y_0(1-A)}{Y} - A \exp \left[-B \left(\tilde{Y} - Y_0 \right) \right]$$

Table 1. *Modified von Mises model***3.1. A residual-type error estimator based on local computations**

The error estimator used in this work was first developed for linear problems [DÍE 98] and later extended to nonlinear problems [HUE 00, DÍE 00]. A detailed presentation and analysis can be found in these references. Here, only a brief review is given.

Using a mesh of characteristic size H , the finite element method provides the discrete nonlinear equilibrium equation

$$\mathbf{f}_H^{\text{int}}(\mathbf{u}_H) = \mathbf{f}_H^{\text{ext}}, \quad [6]$$

where the unknown is the nodal displacement vector \mathbf{u}_H , $\mathbf{f}_H^{\text{int}}(\mathbf{u}_H)$ is the vector of nodal internal forces associated with \mathbf{u}_H and $\mathbf{f}_H^{\text{ext}}$ is the discretized external force term.

To estimate the error in \mathbf{u}_H , a finer mesh of size h ($h \ll H$) is used as reference. On this finer mesh, the problem reads

$$\mathbf{f}_h^{\text{int}}(\mathbf{u}_h) = \mathbf{f}_h^{\text{ext}}. \quad [7]$$

The error in displacements is defined as the difference between the two solutions:

$$\mathbf{e}_u = \mathbf{u}_h - \mathbf{u}_H. \quad [8]$$

Note, however, that computing \mathbf{u}_h is computationally much more expensive than computing \mathbf{u}_H , because it involves solving the nonlinear problem over the fine mesh, see equation [7]. For this reason, the basic idea of the error estimator is to approximate \mathbf{e}_u by low-cost local computations over subdomains. This is a standard strategy in residual-type error estimators.

The proposed approach consists of two phases. First, a simple residual problem is solved inside each element of the coarse mesh (interior estimate). Note that elements are the natural subdomains for the local computations. To avoid the expensive flux-splitting procedures of other residual-type estimators, homogeneous Dirichlet boundary conditions are prescribed for each element (that is, $\mathbf{e}_u = \mathbf{0}$ in the element boundary).

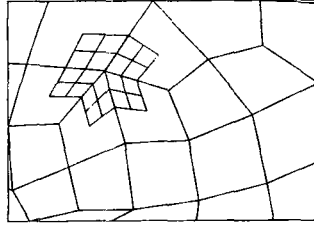


Figure 1. Patch associated to a node of the coarse mesh subdivided into 4×4 elements of the fine mesh

Of course, the error is not really zero in the element boundary. For this reason, a second set of simple problems is solved. The idea is to use a different partition of the computational domain into subdomains. A natural choice is to associate these subdomains, called patches, to the nodes of the coarse mesh. Since four-noded quadrilateral elements are used, a patch consists of one-fourth of each element sharing the node, see figure 1. By combining equations [7] and [8], the nonlinear problem to be solved on every element and every patch can be recast as

$$\mathbf{f}_h^{\text{int}}(\mathbf{u}_H + \mathbf{e}_u) = \mathbf{f}_h^{\text{ext}}. \quad [9]$$

These local problems are solved over the fine mesh of size h . Every element of the coarse mesh H is subdivided into 4×4 elements of size h (i.e. the fine mesh is nested into the coarse mesh, with $h = H/4$). Due to the patch definition, every patch also consists of 4×4 elements of size h , see figure 1. For the iterative solution of equation [9], \mathbf{u}_H is taken as an initial approximation to \mathbf{u}_h (that is, the initial approximation for the error is $\mathbf{e}_u = \mathbf{0}$). This means that the final state obtained with the coarse mesh of size H is taken as the initial state for solving the local problem over each element/patch with the fine mesh of size h .

As a consequence, information must be projected from the coarse mesh H to the fine mesh h . To ensure the consistency between the various projected fields, the following projection strategy is employed: (1) Displacements and damage are projected over the fine mesh. To project the nodal field of displacements, the finite element approximation based on mesh H is used. The damage field must be projected from the Gauss points of the coarse mesh to the Gauss points of the fine mesh. A very simple and efficient strategy is used: the value of damage at each Gauss point of the coarse mesh is assigned to all the Gauss points of the four corresponding elements of the fine mesh, see figure 2. With this projection strategy, the risk of unrealistic values of damage (i.e. $D < 0$ or $D > 1$) is precluded; (2) strains and stresses are not projected, but *computed* from the projected displacements and damage. In this manner, the consistency between all the “projected” quantities (displacements, damage, strains and stresses) is guaranteed. To keep the notation simple, these fields are still denoted with an H subscript denoting they are associated to the solution of the global problem over the mesh of size H , even though they are now supported by the mesh of size h .

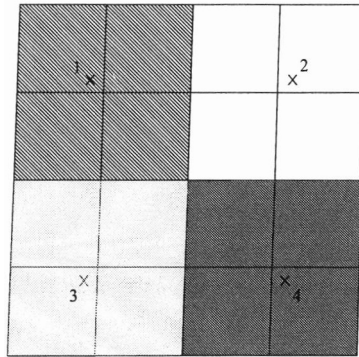


Figure 2. Projection strategy for the damage field. The value at each Gauss point of the element of size H is assigned to the four associated elements of size h

3.2. Accounting for the nonlocality of the model

At this point, it is important to remark that the proposed error estimator for *nonlocal* damage models is based on *local* computations over subdomains (i.e. elements and patches). The nonlocality of the damage model must be accounted for when solving the local problems. Note that, upon mesh refinement, the element size may become smaller than the characteristic length l_c . With the proposed approach, the interaction between adjacent elements is considered (thanks to the loop over patches, that overlap elements), but not the interaction between more distant elements. However, this is not regarded as a significant drawback of the suggested approach; due to the weighting function α of the nonlocal average, see equation [4], the error in one element has a limited influence on the error in distant elements. Moreover, accounting for the interaction between distant elements during the error estimation would destroy the most attractive feature of the suggested approach: it consists of solving *independent* local problems. Note, for instance, that the error estimation algorithm has a computational cost of $\mathcal{O}(N)$ (with N the number of elements) and can be parallelized.

On the other hand, it is essential that these local problems are solved taking into account the current mechanical properties (i.e. the damaged stiffness) of each element/patch. As discussed in the following, this implies that the nonlocal damage model must be slightly modified.

The standard and the modified nonlocal damage models are summarized in table 2. In the standard model—that is, the one used for solving the global problem, see equation [6]—, the error in strains \mathbf{e}_ε is computed as the symmetrized gradient of the error in displacements $\mathbf{e}_\mathbf{u}$ and added to the strains $\boldsymbol{\varepsilon}_H$ to produce the strains $\boldsymbol{\varepsilon}_h$ over the element/patch. After that, the local state variable Y_h is computed and averaged into the nonlocal state variable \tilde{Y}_h . Finally, damage D_h is obtained. Note that the nonlocal average that transforms Y_h into \tilde{Y}_h is over a local support (the element/patch under consideration). This fact leads to non-physical responses, especially in zones

Standard model		Modified model
$\mathbf{e}_\varepsilon = \nabla^s(\mathbf{e}_\mathbf{u})$	Error in strains	$\mathbf{e}_\varepsilon = \nabla^s(\mathbf{e}_\mathbf{u})$
$\varepsilon_h = \varepsilon_H + \mathbf{e}_\varepsilon$	Strain	$\varepsilon_h = \varepsilon_H + \mathbf{e}_\varepsilon$
$Y_h = Y(\varepsilon_h)$	Local variable	$Y_h \approx Y_H + \underbrace{\frac{dY}{d\varepsilon}(\varepsilon_H)\mathbf{e}_\varepsilon}_{e_Y: \text{Error in } Y}$
$Y_h \longrightarrow \tilde{Y}_h$	Nonlocal variable (\longrightarrow : nonlocal average over local support)	$e_Y \longrightarrow e_{\tilde{Y}} \quad ; \quad \tilde{Y}_h = \tilde{Y}_H + e_{\tilde{Y}}$
$D_h = D(\tilde{Y}_h)$	Damage	$D_h = D(\tilde{Y}_h)$

Table 2. Standard and modified nonlocal damage models

of large damage gradients. Assume, for instance, that the error in strains is small and $\varepsilon_h \approx \varepsilon_H$. A small variation in \tilde{Y} is also expected. However, it may happen that $\tilde{Y}_h \ll \tilde{Y}_H$, because \tilde{Y}_h contains no information about nearby zones.

This point is illustrated in figure 3, which depicts the local state variable, the nonlocal state variable and the damage parameter for a given time increment in a zone of the coarse mesh with large gradients. The circled element has a very small local state variable Y_H , see figure 3(a), below the threshold Y_0 . However, since the elements to the right have large values of Y_H , it has a relatively large (above Y_0) nonlocal state variable \tilde{Y}_H , see figure 3(b), which leads to damage, see figure 3(c). If the standard model is used to solve the local problem on the circled element during error estimation, a small error in strains leads to a small variation in the local state variable which, after nonlocal averaging over the element, results in a low value of the nonlocal state variable (that is, $\tilde{Y}_h \ll \tilde{Y}_H$). As a consequence, damage cannot increase in the circled element during error estimation. When estimating the error for the circled element, the nonlocal state variable \tilde{Y}_H , rather than the local state variable Y_H , is representative of its mechanical properties.

For this reason, a modification of the nonlocal damage model is proposed here, see table 2. The difference resides in the way the nonlocal state variable \tilde{Y}_h is computed. By means of a first-order Taylor expansion, the local state variable Y_h is expressed as

Y_H plus an error term e_Y . The derivative $\frac{dY}{d\varepsilon}$ is computed analytically by means of the chain rule

$$\frac{dY}{d\varepsilon_i} = \frac{dY}{dI_1} \frac{I_1}{\varepsilon_i} + \frac{dY}{dJ_2} \frac{J_2}{\varepsilon_i}. \quad [10]$$

In equation [10], ε_i denotes a component of the strain vector. All the derivatives in the RHS are very simple to compute from the definition of the local state variable Y , see table 1 and of the strain invariants I_1 and J_2 .

The error term e_Y is averaged over the element/patch into $e_{\tilde{Y}}$. As a consequence, \tilde{Y}_h is computed as the addition of a reference value \tilde{Y}_H , which describes the real damaged stiffness, and an error term $e_{\tilde{Y}}$. For doing so, it is necessary to project —by means of the same projection strategy used for the damage field, see figure 2— Y_H and $\frac{dY}{d\varepsilon}(\varepsilon_H)$ into the fine mesh.

With this modified model, a small variation in strains does result in a small variation in the nonlocal state variable (that is, $\tilde{Y}_h \approx \tilde{Y}_H$). Going back to figure 3, this means that the damage level of the circled element may either remain constant (for $\tilde{Y}_h < \tilde{Y}_H$) or increase (for $\tilde{Y}_h > \tilde{Y}_H$) during error estimation.

To sum up: the standard model is not capable of capturing the spread of the damaged zone associated to error estimation.

4. Numerical examples: the single-edge notched beam

The proposed adaptive strategy is illustrated here by means of the single-edged notched beam (SENB) test [CAR 93]. The geometry, loads and supports are shown in figure 4. A plane stress analysis is performed. The concrete beam is modelled with the modified von Mises model with exponential damage evolution, see table 1. The steel loading platens are assumed to be elastic. Two sets of material parameters are used, see table 3. For material 1, there is a significant post-peak softening in the stress-strain law for concrete. For material 2, on the contrary, the softening is very slight, so the residual strength almost coincides with the peak strength [PEE 98].

Parameter	Material 1		Material 2	
	Concrete	Steel	Concrete	Steel
E	28 000 MPa	280 000 MPa	35 000 MPa	350 000 MPa
ν	0.1	0.2	0.2	0.2
Y_0	1.5×10^{-4}		6.0×10^{-5}	
A	0.8		0.08	
B	9 000		8 200	
l_c	10 mm		10 mm	

Table 3. The two sets of material parameters: (a) large softening; (b) very slight softening

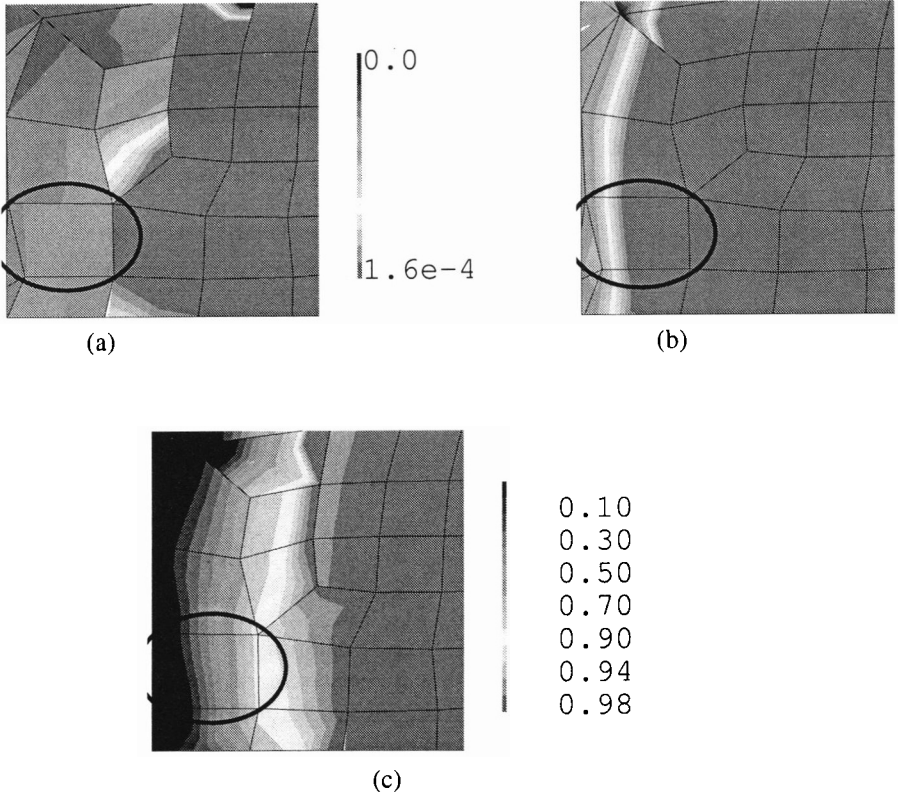


Figure 3. Fields in a zone of large gradients: (a) local state variable Y ; (b) nonlocal state variable \tilde{Y} ; (c) damage. The damage threshold is $Y_0 = 1.5 \times 10^{-4}$

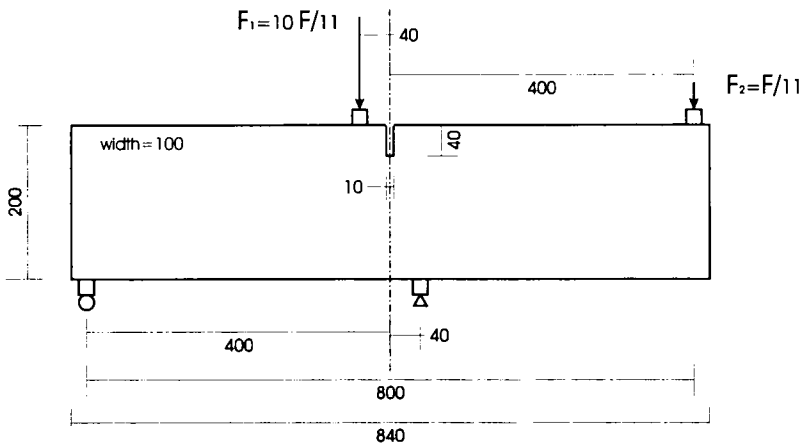


Figure 4. Single-edge notched beam: problem statement. All distances in mm

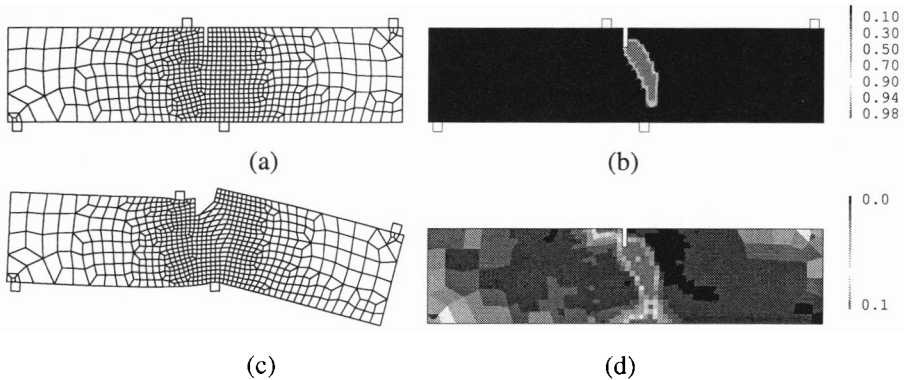


Figure 5. SENB test with material 1, initial approximation in the adaptive process. (a) Mesh 0: 659 elements and 719 nodes; (b) final damage distribution; (c) final deformed mesh ($\times 300$); (d) error distribution. The global relative error is 3.96%

4.1. Test with material 1

The results with material 1 are shown in figures 5 to 7. The initial mesh is shown in figure 5(a). Note that this mesh is relatively coarse, with only one element in the notch width. The final damage distribution and deformed mesh (amplified 300 times), corresponding to a CMSD (crack-mouth sliding displacement) of 0.08 mm, is depicted in figure 5(b). The curved crack pattern observed in experiments [CAR 93] is clearly captured. The error estimation procedure discussed in section 3.2 is employed to compute the error field of figure 5(d). The error is larger in the damaged zone and near the loading platens. The global relative error (i.e. energy norm of the error in displacements over the energy norm of displacements) is 3.96%, above a threshold set a priori of 2%, so adaptivity is required.

The error field of figure 5(d) is translated into the mesh of figure 6(a). Note the element concentration in the crack and the central supports. This finer mesh leads to a better definition of the damaged zone, see figure 6(b). The error estimator now detects that the largest errors are associated to the *edges* of the cracked zone, see figure 6(d). The global relative error of 2.11% is still slightly above the error goal, so another adaptive iteration is performed. The outcome of this second iteration is shown in figure 7. The qualitative results of iteration 1 are confirmed: (1) small elements are needed to control the error in the damaged zones and close to the loading platens and (2) error is larger in the edges than in the centre of the crack. The global relative error of 1.77% is below the threshold of 2%, so the adaptive iterative process stops.

The relation between damage and error is illustrated by figure 8, which depicts profiles of these two fields along the crack. Note that the two error peaks are associated to the edges of the damaged zone (i.e. large damage gradients). This indicates that the damage gradient is a good error indicator [HUE 99] for these models.

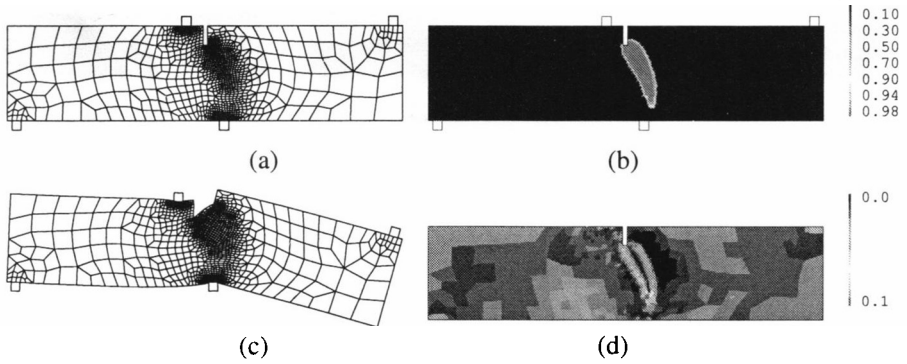


Figure 6. SENB test with material 1, after one iteration in the adaptive process. (a) Mesh 1: 1155 elements and 1228 nodes; (b) final damage distribution; (c) final deformed mesh ($\times 300$); (d) error distribution. The global relative error is 2.11%

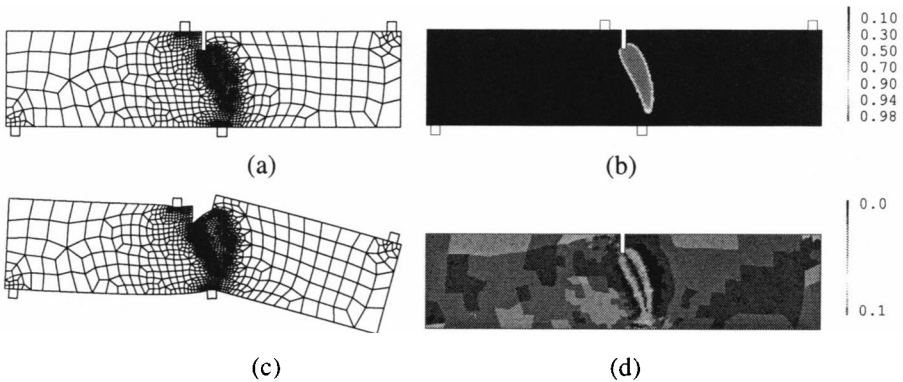


Figure 7. SENB test with material 1, after two iterations in the adaptive process. (a) Mesh 2: 1389 elements and 1469 nodes; (b) final damage distribution; (c) final deformed mesh ($\times 300$); (d) error distribution. The global relative error is 1.77%

4.2. Test with material 2

The SENB test is now reproduced with material 2, see table 3. The small value of parameter A leads to a stress-strain law with almost no softening. A very similar law has been employed to simulate the SENB test with gradient-enhanced damage models [PEE 98].

The results are shown in figures 9 to 11. The initial mesh is the same as before, see figure 9(a). The change in the material parameters lead to a completely different failure pattern, dominated by bending of opposite sign in the two halves of the beam, see figures 9(b) and 9(c). A crack at the notch tip is also initiated, but it is only a

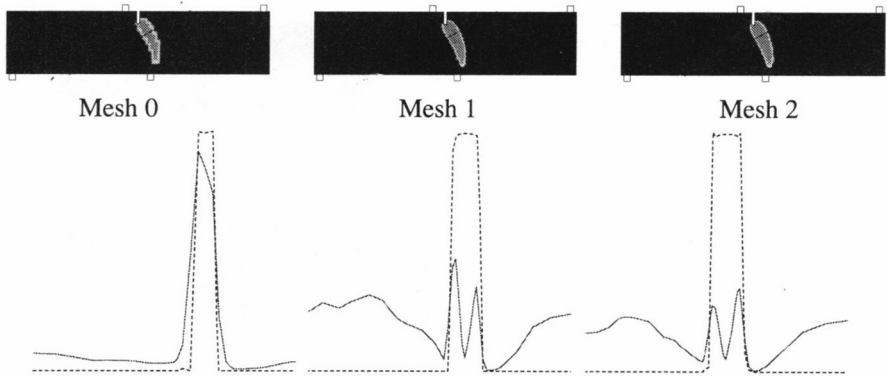


Figure 8. SENB test with material 1. Profiles of damage (dashed line) and error (solid line) across the crack. The two error peaks are associated to large damage gradients

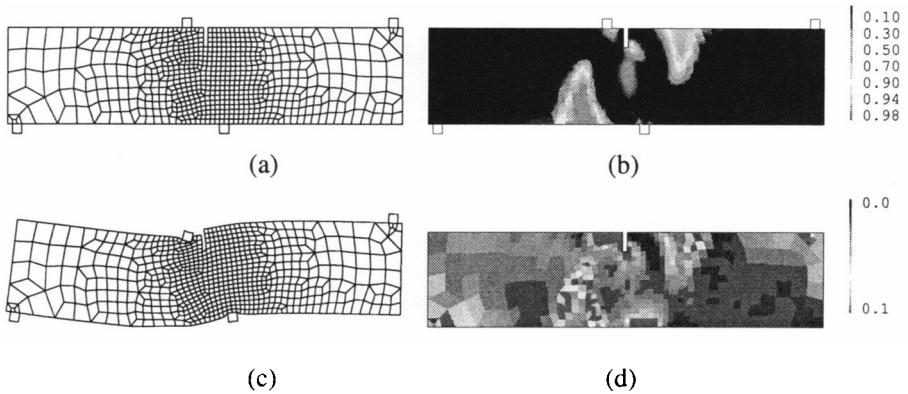


Figure 9. SENB test with material 2, initial approximation in the adaptive process. (a) Mesh 0: 659 elements and 719 nodes; (b) final damage distribution; (c) final deformed mesh ($\times 300$); (d) error distribution. The global relative error is 3.66%

secondary mechanism. The error estimation procedure has no difficulties in reflecting the change in the failure mode, see figure 9(d). The global relative error is 3.66%, so adaptivity is required.

Figures 10 and 11 illustrate the adaptive process. Note that meshes 1 and 2 are quite different from the ones obtained with material 1. The global relative errors are 2.46% and 2.13%. This value is still slightly above the threshold of 2%. However, an additional iteration is considered not necessary for the illustrative purposes of this test.

A final comparison between the two sets of material parameters is offered by figure 12, where the total load is plotted versus the CMSD for meshes 0 and 2. The results

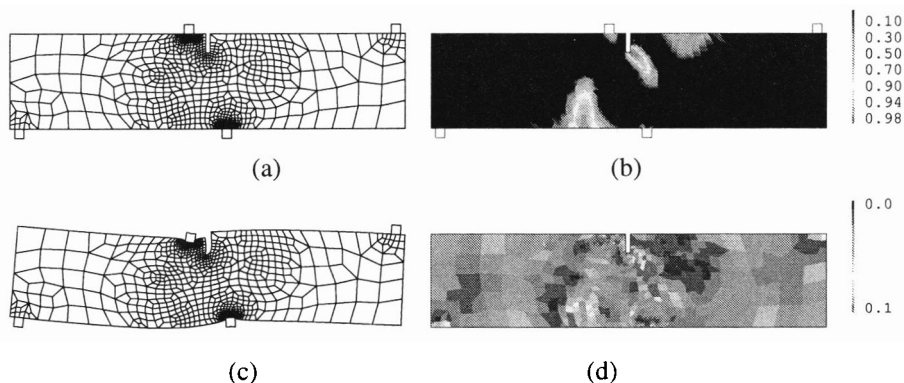


Figure 10. SENB test with material 2, after one iteration in the adaptive process. (a) Mesh 1: 776 elements and 848 nodes; (b) final damage distribution; (c) final deformed mesh ($\times 300$); (d) error distribution. The global relative error is 2.46%

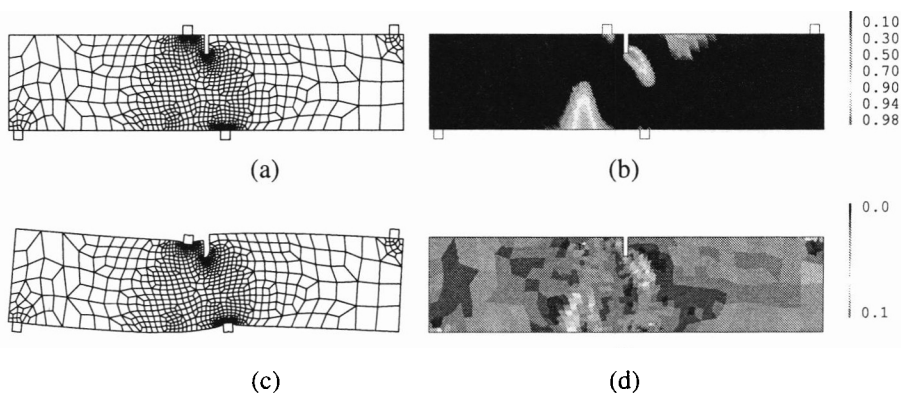


Figure 11. SENB test with material 2, after two iterations in the adaptive process. (a) Mesh 2: 870 elements and 954 nodes; (b) final damage distribution; (c) final deformed mesh ($\times 300$); (d) error distribution. The global relative error is 2.13%

obtained with material 1—a peak load of around 60 kN and post-peak structural softening, see figure 12(a)—are in good agreement with the experiments [CAR 93]. With material 2, on the other hand, the peak load is quite higher and no softening is observed, see figure 12(b).

5. Concluding remarks

An adaptive strategy based on error estimation for nonlocal damage models has been presented. The constitutive model has been slightly modified in order to account for its nonlocality during the error estimation procedure, see table 2. The basic idea

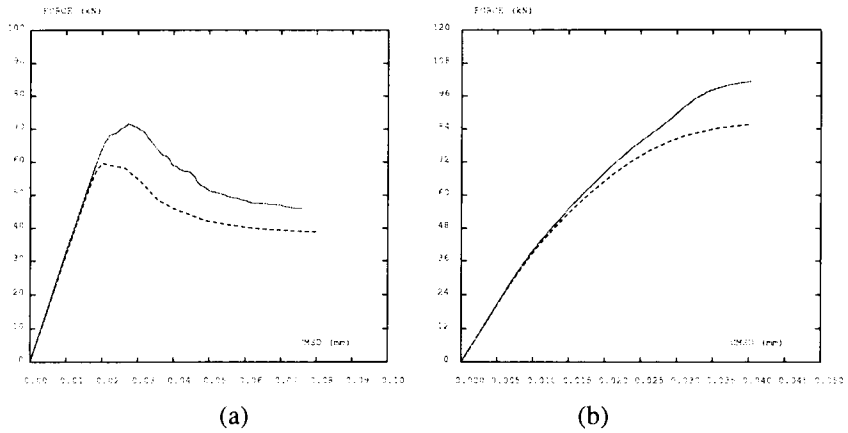


Figure 12. Total load versus crack-mouth sliding displacement (CMSD) for meshes 0 (solid line) and 2 (dashed line): (a) with material 1; (b) with material 2 (see table 3)

of the modification is that the *error* in the local state variable, rather than the variable itself, is averaged. By doing so, the error estimation takes into account the real mechanical properties of the damaged material, while retaining its most attractive feature: it consists in solving simple, independent problems over elements and patches.

The resulting adaptive strategy has been illustrated by means of the single-edge notched beam test. With two sets of material parameters leading to very different failure modes, *h*-remeshing concentrates elements where needed according to the error estimator, until the global relative error falls below an error threshold. By keeping the discretization error under control, it is possible to ensure the quality of the FE solution and assess the influence of the material parameters in an objective way.

Acknowledgements

The partial financial support of the Ministerio de Ciencia y Tecnología (grant numbers: TAP98-0421, 2FD97-1206) is gratefully acknowledged

6. References

- [ASK 00] ASKES H., SLUYS L., "Remeshing strategies for adaptive ALE analysis of strain localisation", *European Journal of Mechanics A/Solids*, vol. 19, 2000, p. 447-467.
- [BAŽ 88] BAŽANT Z., PIIAUDIER-CABOT G., "Nonlocal continuum damage localization instability and convergence", *Journal of Applied Mechanics*, vol. 55, 1988, p. 287-293.

- [BOR 93] DE BORST R., SLUYS L., MÜLHAUS H.-B., PAMIN J., “Fundamental issues in finite element analysis of localization of deformation”, *Engineering Computations*, vol. 10, 1993, p. 99-121.
- [CAR 93] CARPINTERI A., VALENTE S., FERRARA G., MELCHIORRI G., “Is mode II fracture energy a real material property?”, *Computers and Structures*, vol. 48, 1993, p. 397-413.
- [DÍE 98] DÍEZ P., EGOZCUE J., HUERTA A., “A posteriori error estimation for standard finite element analysis”, *Computer Methods in Applied Mechanics and Engineering*, vol. 163, 1998, p. 141-157.
- [DÍE 99] DÍEZ P., HUERTA A., “A unified approach to remeshing strategies for finite element *h*-adaptivity”, *Computer Methods in Applied Mechanics and Engineering*, vol. 176, 1999, p. 215-229.
- [DÍE 00] DÍEZ P., ARROYO M., HUERTA A., “Adaptivity based on error estimation for viscoplastic softening materials”, *Mechanics of Cohesive-Frictional Materials*, vol. 5, 2000, p. 87-112.
- [HUE 99] HUERTA A., RODRÍGUEZ-FERRAN A., DÍEZ P., SARRATE J., “Adaptive finite element strategies based on error assessment”, *International Journal for Numerical Methods in Engineering*, vol. 46, 1999, p. 1803-1818.
- [HUE 00] HUERTA A., DÍEZ P., “Error estimation including pollution assessment for nonlinear finite element analysis”, *Computer Methods and Applied Mechanics in Engineering*, vol. 181, 2000, p. 21-41.
- [LEM 90] LEMAITRE J., CHABOCHE J.-L., *Mechanics of solid materials*, Cambridge University Press, Cambridge, 1990.
- [MAZ 89] MAZARS J., PIJAUDIER-CABOT G., “Continuum damage theory: application to concrete”, *Journal of Engineering Mechanics*, vol. 115, 1989, p. 345-365.
- [PEE 98] PEERLINGS R., DE BORST R., BREKELMANS W., GEERS M., “Gradient-enhanced damage modelling of concrete fracture”, *Mechanics of Cohesive-Frictional Materials*, vol. 3, 1998, p. 323-342.
- [PIJ 87] PIJAUDIER-CABOT G., ZANT Z. B., “Nonlocal damage theory”, *Journal of Engineering Mechanics*, vol. 118, 1987, p. 1512-1533.
- [PIJ 91] PIJAUDIER-CABOT G., MAZARS J., “Steel-concrete bond analysis with nonlocal continuous damage”, *Journal of Structural Engineering*, vol. 117, 1991, p. 862-882.
- [ROD 00] RODRÍGUEZ-FERRAN A., HUERTA A., “Error estimation and adaptivity for nonlocal damage models”, *International Journal of Solids and Structures*, vol. 37, 2000, p. 7501-7528.
- [SAR 00] SARRATE J., HUERTA A., “Efficient unstructured quadrilateral mesh generation”, *International Journal for Numerical Methods in Engineering*, vol. 49, 2000, p. 1327-1350.
- [VRE 95] DE VREE J., BREKELMANS W., VAN GILS M., “Comparison of nonlocal approaches in continuum damage mechanics”, *Computers and Structures*, vol. 55, 1995, p. 581-588.